

# COMPARING FATIGUE LIFE ESTIMATIONS OF COMPOSITE WIND TURBINE BLADES USING DIFFERENT FATIGUE ANALYSIS TOOLS

Oscar Castro<sup>1</sup>, Matthew Lennie<sup>2</sup>, Kim Branner<sup>1</sup>, George Pechlivanoglou<sup>3</sup>, Povl Brøndsted<sup>1</sup>,  
Christian Navid Nayeri<sup>2</sup> and Christian Oliver Paschereit<sup>2</sup>

<sup>1</sup>Department of Wind Energy, Technical University of Denmark  
P.O. Box 49, Frederiksborgvej 399, DK-4000 Roskilde, Denmark  
Email: [osar@dtu.dk](mailto:osar@dtu.dk), [kibr@dtu.dk](mailto:kibr@dtu.dk), [pobr@dtu.dk](mailto:pobr@dtu.dk)

<sup>2</sup>Institut für Strömungsmechanik und Technische Akustik, Technische Universität Berlin  
Müller-Breslau-Straße 8, D-10623 Berlin, Germany  
Email: [matthew.lennie@tu-berlin.de](mailto:matthew.lennie@tu-berlin.de), [christian.nayeri@tu-berlin.de](mailto:christian.nayeri@tu-berlin.de),  
[oliver.paschereit@tu-berlin.de](mailto:oliver.paschereit@tu-berlin.de)

<sup>3</sup>SMART BLADE GmbH  
Zuppingerstraße 14, 88213 Ravensburg, Germany  
Email: [g.pechli@smart-blade.com](mailto:g.pechli@smart-blade.com)

**Keywords:** Composite blade, Fatigue damage, Wind turbine blade

## ABSTRACT

In this paper, fatigue lifetime prediction of NREL 5MW reference wind turbine is presented. The fatigue response of materials used in selected blade cross sections was obtained by applying macroscopic fatigue approaches and assuming uniaxial stress states. Power production and parked load cases suggested by the IEC 61400-1 standard were studied employing different load time intervals and by using two novel fatigue tools called ALBdeS and BECAS+F. The aeroelastic loads were defined through aeroelastic simulations performed with both FAST and HAWC2 tools. The stress spectra at each layer were calculated employing laminated composite theory and beam cross section methods. The Palmgren-Miner linear damage rule was used to calculate the accumulation damage. The theoretical results produced by both fatigue tools proved a prominent effect of analyzed design load conditions on the estimated lifetime of the wind turbine blades and are good starting points for future fatigue analysis using other methods.

## 1 INTRODUCTION

During recent years, wind turbine blades have again exhibited a significant increase in length since wind turbines have changed from mainly being an onshore technology to also being an offshore technology. The associated high investments when installing and operating large modern offshore wind turbines calls for more accurate and reliable lifetime prediction methods for the whole turbine, and for the rotor blades in particular. Often, the fatigue requirement drives the design of these structural members because wind turbines should have an operational life of minimum 20 years. Minimum structural design requirements are specified by the IEC 61400-1 standard [1] and by classification rules and guidelines such as the Germanischer-Lloyd (GL) regulations [2]. However, commonly used lifetime prediction methods suggested by these guidelines, often based on experience from metals, can lead to inaccurate results for the lifetime prediction of composite blades under the strongly varying loads to which they are subjected.

Different fatigue models and life time prediction methodologies have been proposed for analysing fatigue in fibre-reinforced polymers. These models can be generally classified into three categories: the fatigue life models; the phenomenological models for residual stiffness/strength; and the progressive damage models [3]. The first class of *fatigue life models* are based on well-known S-N curves and Constant Life Diagrams (CLD), and have been used to predict fatigue lifetime in fibre-

reinforced composites even when their behaviour is fundamentally different from metals. The second class contains the *phenomenological models* which attempt to describe the effect of fatigue damage evolution in material properties, such as stiffness degradation and strength degradation, in terms of macroscopically observable properties. The third class of *progressive damage models* differ from previous models in that they introduce one or more properly chosen damage variables which describe directly the deterioration of the composite component.

Several authors have addressed issues related to fatigue behaviour and life prediction of wind turbine composite blades by using *fatigue life models* [4-7]. Sutherland and Kelley [4] analysed the effect of mean stress on the prediction of damage from the typical wind turbine load spectra using CLDs for characterizing the behaviour of composites used in wind turbine blades. Kong et al. [5] estimated the fatigue life for operating more than 20 years of an E-glass/epoxy composite blade for a medium-scale horizontal axis wind turbine by using the S–N linear damage equation, an empirical load spectrum and Spera’s empirical formulae [8]. Jang et al. [6] developed an fatigue life prediction method by introducing the concept of probabilistic *S-N (P-S-N)* curves, and studied the effect that 10-min mean wind speed distribution has on the fatigue life of small-scale wind turbine composite blade. Nijssen [7] studied the fatigue life prediction of composite wind turbine rotor blades by comparing Miner’s sum method and strength-based life prediction. Few authors have applied *progressive damage models* for life prediction of wind turbines. Cárdenas et al [9], for example, introduced a computational platform which provides a real-time analysis of the damage progression in wind turbine blades under realistic wind and operational conditions. Even though these studies presented positive results for the fatigue of composite blades in different ways, it is still necessary to continue the study of fatigue behaviour of composite blades whose behaviour is strongly affected by several factors such as inherent defects (e.g. manufacturing wrinkles, fibre misalignments and voids), structural architecture, and loading conditions.

This paper presents an initial study made to continue understanding the fatigue behaviour of composite wind turbine rotor blades. For this purpose, the NREL 5 MW reference wind turbine rotor was analysed using two novel fatigue tools that predict fatigue lifetime of rotor blades following *fatigue life models* described by current guidelines. The first tool is ALBdeS, an extension of the 2D sectional analysis tool PMV developed by Smart Blade GmdH, and the second one is BECAS+F, an extension of the beam cross section BECAS software developed by DTU Wind Energy, which is capable of predicting fatigue life of rotor blades under different loading conditions. Based on above tools, the fatigue life of materials used in different blade cross sections were obtained taking into account a combination of normal design situations and different simulated load time intervals.

## 2 GENERAL BLADE DESIGN CONSIDERATION

The NREL 5 MW reference wind turbine, which is representative of utility-scale multi-megawatt turbines, was considered in this study. This wind turbine is a conventional three-bladed upwind variable-speed, variable blade-pitch-to-feather-controlled turbine [10]. Table 1 gives the general properties of this turbine.

Rating	5 MW
Wind regime	IEC 61400-1 (Onshore) Class 1B
Rotor orientation/Configuration	Upwind/3 blades
Control	Variable speed, collective pitch
Rotor diameter/Hub diameter	126 m / 3m
Hub height	90 m
Maximum rotor/generator speed	12.1 / 1173.7 rpm
Maximum tip speed	80 m/s
Overhang/Shaft tilt/Precone	5m / 5°/ 2.5°
Rotor/ Nacelle/Tower mass	110000 kg/240000 kg/347460 kg

Table 1: General properties of the NREL 5-MW baseline wind turbine [10].

The blades of the NREL reference turbine model are 61.5m long and weigh 17740kg each. The distributed structural properties of these blades were described by Jonkman [10] and a basic structural layup concept was proposed by Resor [11]. This blade structural concept was suggested to provide a starting point for more details and targeted investigations related among others with blade design tool verification and material and structural studies. In this sense, cross sections and chord schedules used in present study were taken from Jonkman [10], and almost all material properties and skin layups from Resor [11].

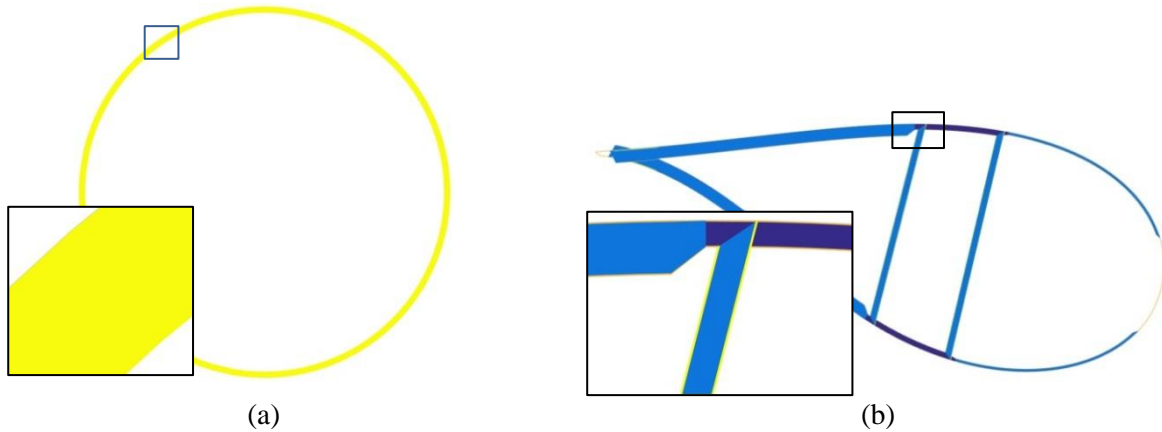


Figure 1: Shapes and layups of evaluated cross sections: (a) blade root; (b) 10.5m blade span.

Fig.1 shows the cross section shapes of blade root and 10.5m blade span, which were analysed in current study. They were chosen to compare the ability of the implemented fatigue methods (which will be described in further sections) to predict fatigue life in cross sections with simple and more complex shapes and layups. In addition, 10.5m blade span is also interesting because it is subjected to a highly critical fatigue behaviour, according to Resor [11] and Castro et al. [12]. Blade root section is characterized by a circular cross section with a diameter of 3.386m, while blade span at 10.25m from the root has a DU W-405 airfoil shape, a chord length of 4.557m and twist of 13.308°. More details about the blade station parameters can be found in references [10, 11].

No	Material	Thickness (mm)	$E_x$ (GPa)	$E_y$ (GPa)	$G_{xy}$ (GPa)	$\nu_{xy}$ (-)	$\rho$ (kg/m <sup>3</sup> )	$X_t$ (MPa)	$X_c$ (MPa)
1	Glass(UD) <sup>a</sup>	0.47 <sup>b</sup>	39.4	15.14	5.5	0.29	-	793.05	542.49
2	SNL(Triax)	0.94	27.70	13.65	7.20	0.39	1850	700	-
3	Saertex(DB)	1	13.60	13.30	11.80	0.49	1780	144	213
4	Carbon(UD)	0.47	114.50	8.39	5.99	0.27	1220	1546	1047
5	Foam	1	0.26	0.26	0.022	0.3	200	-	-
6	Gelcoat	0.05	3.44	-	1.38	0.3	1235	-	-

Table 2: Mechanical properties of materials. <sup>a</sup> Obtained from Passipoularidis et al. [13]. <sup>b</sup> This value was assumed.

No	Material	$\gamma_{Ma}$ (-)	$C_{2b}$ (-)	$C_{3b}$ (-)	$C_{4b}$ (-)	$C_{5b}$ (-)	$m$ (-)
1	Glass(UD)	2.65	1.1	1.0	1.1	1.2	10
2	SNL(Triax)	2.65	1.1	1.2	1.1	1.2	10
3	Saertex(DB)	2.65	1.1	1.2	1.1	1.2	10
4	Carbon(UD)	2.65	1.1	1.0	1.1	1.2	14
5	Foam	-	-	-	-	-	-
6	Gelcoat	-	-	-	-	-	-

Table 3: Fatigue partial safety factors for the materials.

Table 2 summarizes the mechanical properties of materials implemented in this study. Almost all of them were adopted from [11] excepting the E-LT-5500(UD) material, which was replaced by a Glass(UD) from [13], in order to obtain a well-characterized material to make further multiaxial an non-linear fatigue analyses. Adhesive is not taken into account as perfect bonding is assumed. The partial safety factors for all material, shown in Table 3, were derived according to GL guidelines [2].

Fig. 1 also shows an example of the stacking sequences implemented in the different blade airfoil section regions (i.e. Upper Trailing Edge, the Upper Spar Cap, Leading Edge, etc.), whose detail information can be found in [11]. A redesign of shear web layups was made in order to reduce possible fatigue failures in the webs, as were shown in [12]. The redesign consisted in adding two layers of double bias (DB) material, Saertex(DB), in each web face for a total of 4 mm of DB, see Table 4.

<i>Blade span</i> (m)	<i>Material stack</i>	<i>No of layer of</i> <i>DB per stack</i>	<i>Foam thickness</i> (mm)
10.5	<i>Saertex(DB), Foam, Saertex(DB)</i>	4	50

Table 4: Stack usage in shear webs

### 3 FATIGUE LOAD CASES

The NREL 5MW reference wind turbine was analysed based on wind class IB, according to the IEC61400-1 standard [1]. The IEC61400-1 standard describes five design load cases in which the primary concern is the fatigue loading which makes up its life time (20 years). Power production (DLC 1.2) and parked (DLC 6.4) condition were analysed in this study and controller dependent design cases (DLC2.4, DLC3.1, DLC4.1) were omitted since these events are highly controller depending. Table 5 presents the general information for the evaluated design load cases.

Design situation	DLC	Wind condition
Power production	1.2	NTM*, $V_{in} < V_{hub} < V_{out}$
Parked (standing still or idling)	6.4	NTM, $V_{hub} < 0.7V_{ref}$

Table 5: Evaluated fatigue load cases. \*Normal Turbulence Model

### 4 AEROELASTIC TURBINE MODELS

The aeroelastic simulations were developed using both FAST [14] and HAWC2 [15] tools in order to establish confidence in the predictive capabilities of implemented fatigue methods, which will be described in next section. Both aeroelastic tools have been extensively used to analyze the response in the time domain of a range of wind turbine configurations (including two- or three-blade horizontal-axis rotor, pitch or stall regulation, rigid or teetering hub, and upwind or downwind rotor), by joining aerodynamics models, control and electrical system (servo) dynamics models, and structural (elastic) dynamics models. A comparison between the aero-hydro-servo-elastic capabilities of these two codes can be found in [16].

The main input parameters for the aeroelastic simulations are presented in Table 6. According to IEC61400-1 the standard [1], a set of wind speeds following Rayleigh distribution (with parameters  $a = 2$  and  $b = \sqrt{4/\pi} (0.2V_{ref}) = 11.2827 \text{ m/s}$ ) were evaluated for each DLC case: wind speeds from 3 to 25 m/s with a 2 m/s step for the DLC 1.2 case, and wind speeds from 3 to 35 m/s with the same step for DLC 6.4 case. Just one yaw case of  $0^\circ$  was analyzed. Each case above is to be modelled with one turbulence seed for each 10 minutes series. Finally, effects of all DLC conditions were scaled with proper weighting factors.

Rating	5 MW
Wind regime	IEC 61400-1 (Onshore) Class IB
Rotor orientation/Configuration	Upwind/3 blades
Control	Variable speed, collective pitch
Rotor diameter/Hub diameter	126 m / 3m
Hub height	90 m
$V_{in} / V_{cut} / V_{rated}$	3 m/s / 25 m/s / 11.4 m/s
$V_{ref}$	50 m/s
Average wind speed	$0.2 * V_{ref} = 10m/s$
$V_{50}$	$1.4 * V_{ref} = 70m/s$
$V_1$	$0.8 * V_{50} = 56m/s$
Mean turbulent speeds for DLC 1.2 case	3m/s-25 m/s every 2 m/s
Mean turbulent speeds for DLC 6.4 case	3m/s-35 m/s every 2 m/s
Yaw error	0°
Number of seeds	1
Turbulence model	Von Karman
Aeroelastic simulation usable record length	700 sec (First 100 sec discarded for transitorily behaviour)
Time step	0.0125 sec
Turbine design life	20 years

Table 6: Important input parameters for aeroelastic simulations [10].

## 5 FATIGUE LIFETIME PREDICTION

The estimation of fatigue life based on the so-called *fatigue life models* was developed using both ALBdeS and BECAS+F codes. ALBdeS (ALBert BLAde Simulation, named after W. Albert the first author to write a paper considering fatigue) is an extension of the PMV custom section rotorblade analysis tool of SMART BLADE GmbH [12]. ALBdeS tool calculates the cumulative damage value in each individual layer of the blade section laminates and determines whether or not failure will occur over the course of 20 years under power production conditions (i.e. DLC 1.2). Meanwhile BECAS+F, which is an extension of BECAS (BEam Cross section Analysis Software) developed by DTU Wind Energy [17], also computes the cumulative damage and fatigue lifetime of rotorblade cross sections but taking into account the effects of different load conditions (e.g. DLC 1.2 and DLC 6.4).

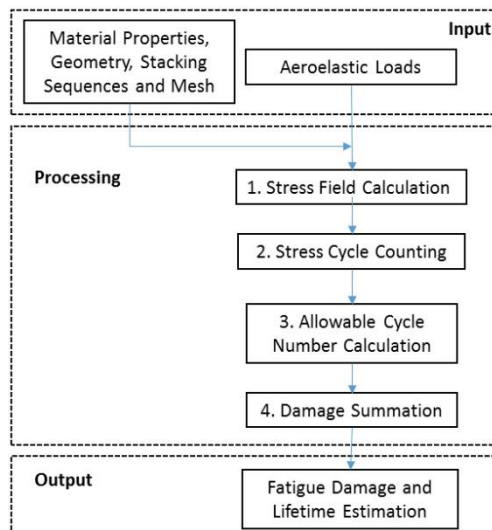


Figure 2: General fatigue life prediction methodology implemented by both ALBdeS and BECAS+F codes.

The flowchart presented in Fig. 2 shows the general procedure followed by both tools to predict fatigue lifetime of rotor blades, which is based on GL guidelines [2]. Information regarding the cross section (i.e. material properties, cross section shape, stacking sequences and finite element mesh) and the aeroelastic local span loads (i.e. flapwise, edgewise, pitch and axial loads (forces and moments)) is required as input data. ALBdeS takes the cross section information from PMV, which is a code that implements various beam theories to calculate sectional characteristics of a given cross section and recovers the displacement/strain/stress distribution within the structure. BECAS+F, as an extension of BECAS tool, takes the cross section input from Airfoil2BECAS [18], which is a set of python functions that allow for the generation of input files for the analysis of a wind turbine blade cross-section with BECAS. ALBdeS was designed to take aeroelastic loads from FAST and BECAS+F from HAWC2, but both fatigue codes can process load information from both aeroelastic tools.

The first step during the processing is the stress field calculation. For this purpose, ALBdeS selects as time interval  $\Delta t$ , during which fatigue cycles will be evaluated, equal to time taken for one rotor revolution. The selected rotor revolution is taken randomly (using random function of python) from the 10min-simulated-aeroelastic data. All cycles per load into the selected  $\Delta t$  are extracted and discretized in  $n$  points to obtain load vectors ( $\mathbf{F}_{n(PVM)} = [F_{a,n} \ F_{e,n} \ F_{f,n} \ M_{p,n} \ M_{f,n} \ M_{e,n}]$ ) for each time instant, which are introduced one by one in PMV to compute the stress fields. Fig. 3 shows a schematic representation of this process, which is described in detail in [12]. BECAS+F, on the other hand, discretizes the whole simulated time series (i.e.  $\Delta t = 10$  min) by defining either  $n$  points per rotor revolution or a fixed time step for all simulated cases. Each load data in vector shape ( $\mathbf{F}_{n(BECAS)} = [F_{e,n} \ F_{f,n} \ F_{a,n} \ M_{f,n} \ M_{e,n} \ M_{p,n}]$ ) per time instant is processed by BECAS to obtain the stress fields.

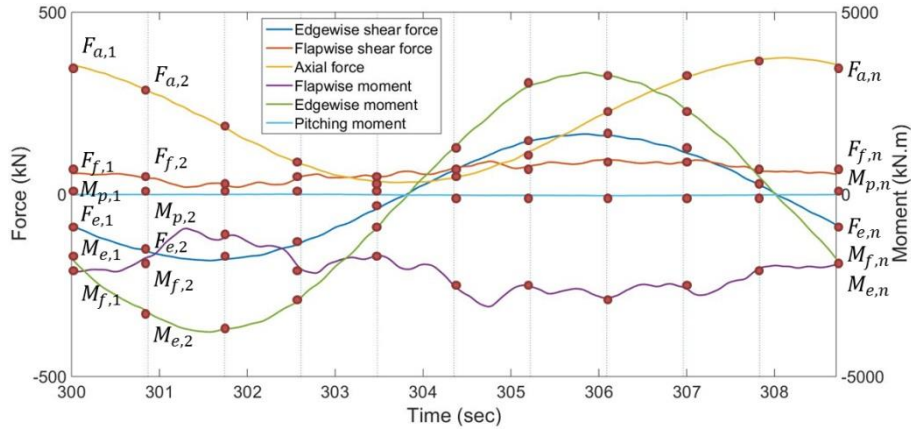


Figure 3: Selected load cycles into a time interval,  $\Delta t$ , and  $n$  divisions to obtain the load vectors to be analyzed by PMV.

The second step during the procedure is the stress cycle counting to convert variable amplitude time series of normal stress cycles into blocks of certain numbers of cycles,  $n$ , that correspond to constant amplitude and mean values. For this purpose, both fatigue tools have implemented Rainflow Cycle Counting Method according to [2]. ALBdeS uses Crunch post-processing code developed by NREL [19] and BECAS+F employs the Rainflow algorithm prepared for using in the MATLAB® environment [20]. In both cases all unclosed cycles are treated as half cycles, according to [20].

The third step is the calculation of allowable cycles,  $N$ . Both fatigue tools use CLDs, which show the relationship between the mean and the range components of the normal stresses,  $\sigma_{1,m}$  and  $\sigma_{1,a}$ , and the traction and compression strengths,  $X_t$  and  $X_c$ . The number of allowable cycle can be found then as follows:

$$N = \left[ \frac{X_t + |X_c| - |2\gamma_{M_a} \sigma_{1,m} - X_t + |X_c||}{2(\gamma_{M_b} / C_{1b}) \sigma_{1,a}} \right]^m \quad (1)$$

The last step in the lifetime prediction is the calculation of the damage accumulation,  $D_y$ . Both ALBdeS and BECAS+F compute this value utilizing linear Palmgren-Miner rule [21, 22] and taking into account all operating states and all stress levels during the wind turbine lifetime (see Eq. 2), according to [23].

$$D_y = D_{y,O} + D_{y,P} + D_{y,T} \quad (2)$$

Where the cumulative damage for transitional conditions,  $D_{y,T}$ , is omitted in the present study and cumulative damages for normal operation and parked conditions,  $D_{y,O}$  and  $D_{y,P}$ , may be calculated as follows:

$$D_{y,(O,P)} = \sum_{i=V_{in}}^{V_{(out,max)}} C \sum_j \sum_k F_{V_i} \frac{n(\sigma_{1,m,j}, \sigma_{1,a,k}, V_i \Delta t)}{N(\sigma_{1,m,j}, \sigma_{1,a,k})} \quad (3)$$

where  $C$  is the total number of time intervals per 20 years;  $i$  is the index for wind speeds (incremented from cut-in to cut-out wind speed for normal operation cases and from cut-in to max wind speed for parked cases);  $j$  is the index for mean stress level (covering the range of mean stress levels encountered);  $k$  is the index for stress amplitude (covering the range of all stress amplitudes encountered);  $\Delta t$  is the length of the time interval during which fatigue cycles are evaluated;  $V_i$  is the free stream wind speed; and  $F_{V_i}$  is the probability density of  $V_i$  which depends also on the Rayleigh parameters  $a$  and  $b$ :

$$F_{V_i} = \frac{a}{b} \left(\frac{V_i}{b}\right)^{a-1} e^{-\left(\frac{V_i}{b}\right)^a} \quad (4)$$

As an output, ALBdeS and BECAS+F give the cumulative damage and lifetime prediction of each material from a given blade cross section. The fatigue lifetime prediction is computed as  $20/D_y$ . As a summary, Table 7 presents a comparison between ALBdeS and BECAS+F tools.

	<b>ALBdeS</b>	<b>BECAS+F</b>
Code developer	SMART BLADE GmbH	DTU Wind Energy
<b>Input</b>		
Cross section information	PMV	Airfoil2BECAS
Aeroelastic local span loads	FAST (or other aeroelastic tool)	HAWC2 (or other aeroelastic tool)
<b>Processing</b>		
Stress field calculation	a) PMV tool b) From one rotor revolution into 10-min simulation c) Under power operation conditions (DLC 1.2)	a) BECAS tool b) From whole 10-min simulation c) Under power operation and parked conditions (DLC 1.2 and DLC 6.4)
Stress cycle counting	a) Rainflow method b) Crunch tool	a) Rainflow method b) Rainflow algorithm for MATLAB <sup>®</sup>
Allowable cycle calculation	CLDs	CLDs
Damage summation	Linear Palmgren-Miner rule	Linear Palmgren-Miner rule
<b>Output</b>		
Fatigue output	Damage and total lifetime of given cross section	Damage and total lifetime of given cross section

Table 7: Overview of fatigue modeling capabilities of ALBdeS and BECAS+F codes

## 6 FATIGUE SETUP CASES

Table 8 presents a description of the five evaluated cases, which were proposed to establish confidence in the predictive capabilities of implemented fatigue methods and to analyze the effect of different load conditions on the total fatigue lifetime of the studied cross sections (i.e. blade root and 10.5 span section).

Case	Fatigue tool	Aeroelastic tool	DLC	$\Delta t$ (min)	$C$
1.	ALBdeS	FAST	1.2	$1/\omega_{rotor}$	$10.512E6/\Delta t$
2.	BECAS+F	FAST	1.2	$1/\omega_{rotor}$	$10.512E6/\Delta t$
3.	BECAS+F	FAST	1.2	10	$10.512E6/\Delta t$
4.	BECAS+F	HAWC2	1.2	10	$10.512E6/\Delta t$
5.	BECAS+F	HAWC2	1.2 (60%) + 6.4 (40%)	10	$10.512E6/\Delta t$

Table 8: Different cases evaluated

According to a sensitivity study, the stress fields for all cases were obtained discretizing the load cycles for each rotor revolution into 30 points. For cases 1 and 2, the same rotor revolution data was analysed in each wind speed. For case 5, an operation time of 60% throughout the estimated life-span of 20 years was assumed (which matches with lifetime expectations of novel wind turbines [24]) and the remaining time as parked conditions.

## 7 RESULTS AND DISCUSSIONS

### 7.1 Aeroelastic loads

Fig. 4 show an example of comparison between aeroelastic loads (forces and moments) obtained from both FAST and HAWC2 aeroelastic tools. In general, the two simulation tools compare well. Some differences can be observed regarding to mean values and number of high frequency cycles due possibly to the implementation of aerodynamic induction, tower interference, hub and tip loss, and dynamic stall models, as explained in [25]. The possible effects of these differences on fatigue life predictions can be analyzed easier from Fig. 5, which shows examples of variations between number of cycles/mean load/load amplitudes ratio from different aeroelastic loads obtained from both FAST and HAWC.

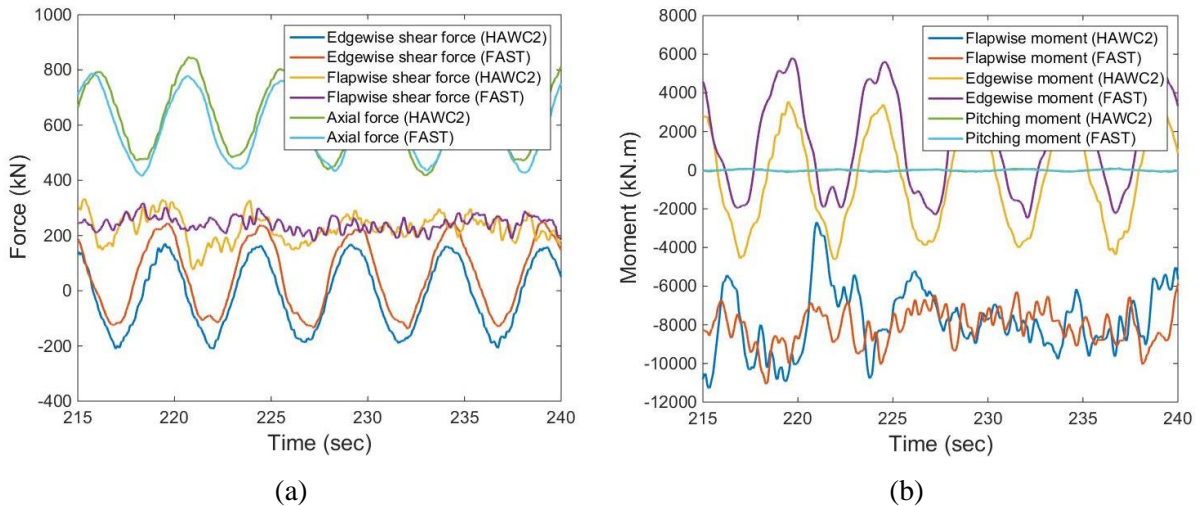


Figure 4: Aeroelastic loads at blade root for a wind speed of 13 m/s and DLC 1.2, obtained from FAST and HAWC2 tools. (a) Forces; (b) Moments

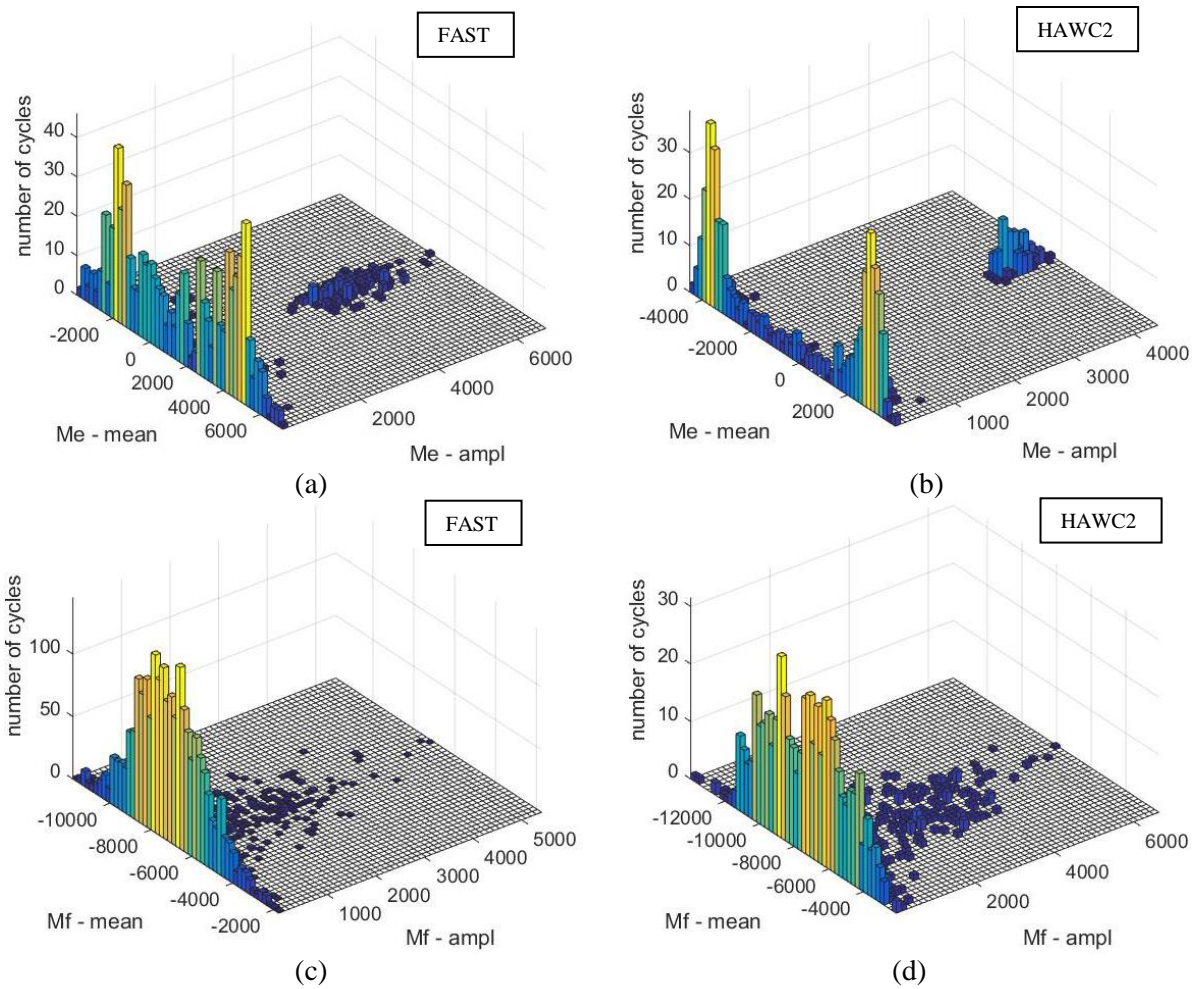


Figure 5: Rainflow cycle counting of edgewise (a-b) and flapwise (c-d) moments time series from 10-min simulations for a wind speed of 13 m/s and DLC 1.2, obtained from FAST and HAWC2

Fig. 6 gives an example of aeroelastic loads from parked conditions (DLC 6.4), obtained by using HAWC2. It is possible to observe how the rotor continues rotating with a low angular speed even the turbine is parked.

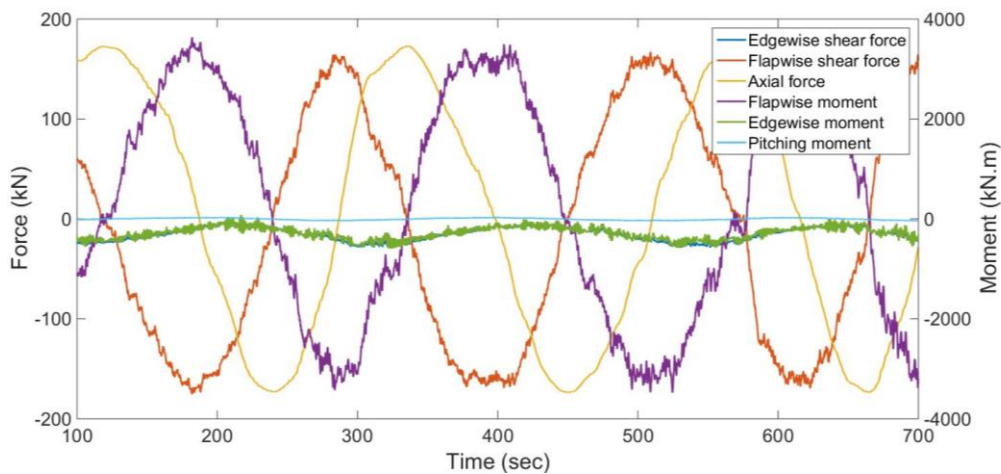


Figure 6: Aeroelastic loads at blade root for a wind speed of 13 m/s and DLC 6.4, obtained from HAWC2.

## 7.2 Fatigue lifetime prediction

Table 9 shows the predicted fatigue lifetime for the blade root and the 10.5m blade span section for all evaluated cases listed in Table 8. In general, total fatigue lifetime at the root is much higher than at the 10.5 blade span section, which match well with results obtained in [11, 12]. Even though shear webs at 10.5 blade span section were redesigned in this study, failure caused by fatigue is likely to happen at this section with a short lifetime according to the predictions.

	<i>Fatigue life (years)</i>	
	<i>Blade root</i>	<i>10.5 blade span section</i>
Case 1	8.2E+08	3.1E+00
Case 2	3.4E+08	6.3E-01
Case 3	1.5E+08	2.5E+00
Case 4	9.9E+07	4.9E+00
Case 5	1.6E+08	8.1E+00

Table 9: Fatigue lifetime prediction for blade root and 10.5m blade span, for all evaluated cases.

Cases 1 and 2 compare the results from the ALBdeS and BECAS+F codes using the same load spectrum data (see Table 8). Even stress field obtained from PMV and BECAS match well for simple shapes and layups as presented at blade root (see Fig. 7-a), differences between fatigue life predictions from both fatigue tools can be observed. These dissimilarities are mainly generated during the rainflow stress cycle counting step. As shown in Fig. 7-b, elements located in the same position at blade root from PVM and BECAS's meshes present different mean stress/stress amplitude ratio, being some of them more critical than others. This causes a significant variation of the predictive accumulative damage from both fatigue tools; which, for example, is around 25.7% for the mesh element that is being analysed in Fig. 7-b. In addition, the cross section mesh also could affect the fatigue prediction when cross section shapes and layups become more complex because the mesh generation is more difficult to manipulate using both PVM and Airfoil2BECAS tools. For example, the number of elements that PVM uses to discretize a laminate is equal to its own number of layers, while for Airfoil2BECAS, the minimum value for discretizing any laminate is the largest number of layers of different material anywhere in the cross section. This could generate even more discrepancies between both fatigue tools as shown in results obtained for 10.5 blade section span.

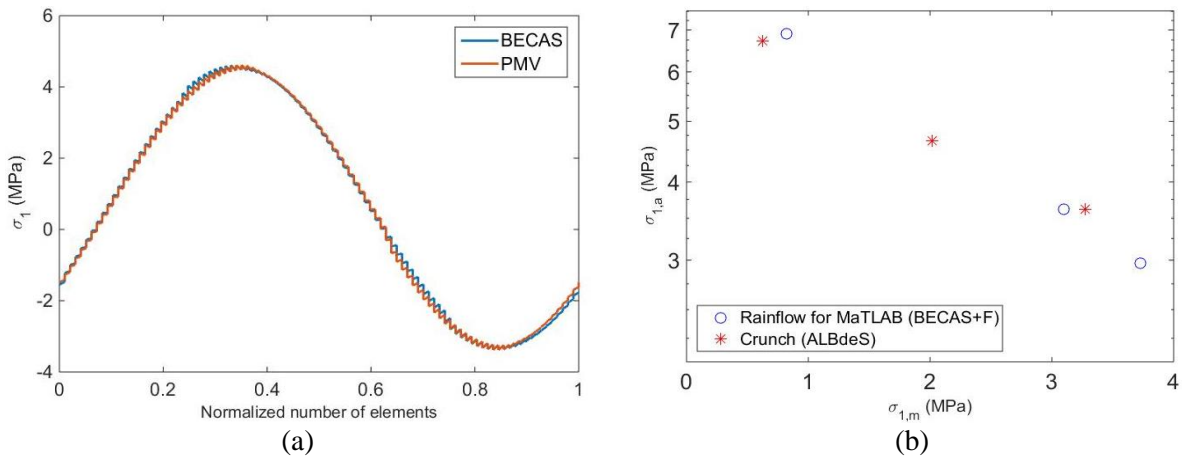


Figure 7: (a) Stress field at blade root for a wind speed of 3m/s and DLC 1.2 ( $\mathbf{F} = [F_e \ F_f \ F_a \ M_f \ M_e \ M_p] = [-38.18 \ 58.42 \ 368.20 \ -1803.00 \ -768.10 \ -12.06]$  N); (b) Rainflow cycle counting of  $\sigma_1$  series from a mesh element located in  $x = -1.6649$  m and  $y = 0.2848$  m, using both Rainflow algorithm for MATLAB<sup>®</sup> and Crunch. Wind speed of 3m/s and DLC 1.2. Predicted damage accumulation of the element:  $D_{y(ALBdes)} = 5.590572e - 11$  and  $D_{y(BECAS+F)} = 7.522700e - 11$

Comparing cases 2 and 3 allows discussing the effects of (a) taking load cycles from one rotor revolution ( $\Delta t = 1\text{min}/\omega_{\text{rotor}}$ ) and projecting their outcomes (stress fields) throughout the estimated life-span of 20 years, and (b) projecting the stress fields from a 10min-aeroelastic simulation ( $\Delta t = 10\text{min}$ ) onto the 20 years life-span. The estimated lifetime from case 2 could be lower or higher than that from case 3 (as shown in blade root and 10.5 blade span, respectively) because the load data contained in one single rotor revolution can become more or less critical depending on the selected rotor revolution.

Cases 3 and 4 compare results obtained processing loading data from both FAST and HAWC2 aeroelastic tools. As shown, the aeroelastic simulation differences described in Section 7.1 regarding to cycles/mean load/load amplitudes ratio can also affect significantly the fatigue life prediction of rotor blades. Finally, case 4 and 5 show the effects of taking into account different design load conditions. An increase of lifetime is predicted when parked conditions are considered together with power production conditions. This is caused by the effects of both low load mean values and low frequency cycles related with the low rotor speed in DLC 6.4 cases, (see Fig. 6).

On the other hand, Table 10 shows the lifetime for each material used at 10.5m cross section. In this particular layout, unidirectional carbon fiber layers used in spar caps hold up well against the fatigue loads; however, those made of unidirectional glass fibers, which are implemented in reinforced trailing edges, appear to be under designed. A relative lifetime increment of layers made of Saertex(DB), which are used in shear webs, was obtained with the redesign proposed in this study, becoming less critical than layers made of Glass(UD).

	<i>Fatigue life (years)</i>			
	<i>Glass(UD)</i>	<i>SNL(Triax)</i>	<i>Saertex(DB)</i>	<i>Carbon(UD)</i>
Case 1	3.1E+00	2.5E+02	2.7E+03	1.4E+05
Case 2	6.3E-01	1.0E+02	3.6E+03	1.7E+05
Case 3	2.5E+00	2.4E+02	2.9E+02	4.6E+04
Case 4	4.9E+00	3.4E+02	5.0E+01	8.1E+04
Case 5	8.1E+00	5.7E+02	8.4E+01	1.4E+05

Table 10: Fatigue lifetime prediction for the 10.5m cross section, for all evaluated cases. Material 1: *Glass (UD)*; Material 2: *SNL(Triax)*; Material 3: *Saertex(DB)*; Material 4: *Carbon(UD)*

The effects of the rainflow cycle counting process and cross section meshing on the fatigue lifetime estimations are also showed Table 10, where high dissimilates between cases 1 and 2 are presented for all materials. The material response can be also affected by variations of load input data. Predicted lifetimes from cases 1 and 2 (load data from one rotor revolution) are lower than those from cases 3 and 4 (load data from 10min simulation) for materials 1 and 2, and higher for materials 3 and 4. In addition, the effects of differences between aeroelastic loads from cases 3 and 4 (load data from FAST and HAWC2, respectively) are also shown, especially for Saertex(DB) layers. The above described material response variations should also be related with the layer location in the cross section. For example, Saertex(DB) material is only used in shear webs, whose response are highly affected by variations in shear forces. Finally, a general increase in lifetime is predicted for most of the materials when power production and parked conditions are taking into consideration.

## 8 CONCLUSIONS

Fatigue lifetime of blade root and 10.5 blade section of the NREL 5MW reference wind turbine were predicted in this study by using two novel fatigue tools called ALBdeS and BECAS+F. The fatigue response of the blade sections was obtained applying *fatigue life models* described by Germanischer-Lloyd (GL) regulations. Power production and parked load cases suggested by the IEC 61400-1 standard were studied. Aeroelastic simulations through FAST and HAWC2 tools were developed to obtain the aeroelastic loads. The stress spectra at each layer were calculated employing laminated composite theory and beam cross section methods. The rainflow cycle counting method was

implemented to analyse the uniaxial stress series and the Palmgren-Miner linear damage rule was used to calculate the accumulation damage.

The comparison between the two tools indicates to the authors that different implementations of the same method can show fairly significant deviations on fatigue life predictions. These dissimilarities were caused by different factors: (a) the rainflow cycle counting algorithm implemented for each fatigue tool; (b) the cross section meshing, especially for complex cross section shapes and layups; (c) discrepancies between aeroelastic loads calculated by the different aeroelastic tools; and (d) the time interval during which fatigue cycles were evaluated. In addition, an increase of lifetime was obtained when both power production and parked load conditions were considered.

The results found in this study give a good background for a further understanding of the different factors that affect the analytical fatigue life prediction in wind turbine blades and for predictions using improved fatigue models.

## REFERENCES

- [1] IEC, "Wind Turbines " in *Part 1. Design Requirements*, ed, 2005-2008, p. 92.
- [2] GL, "Rules and Guidelines," in *Guideline for the Certification of Wind Turbines*, ed. Hamburg: Germanischer Lloyd, 2010, p. 384.
- [3] J. Degrieck and W. Van Paepegem, "Fatigue damage modeling of fibre-reinforced composite materials: Review," *Applied Mechanics Reviews*, vol. 54, p. 22, 2001.
- [4] H. J. Sutherland and N. D. Kelly, "Fatigue damage estimate comparisons for Northern European and U.S. wind far loading environments," presented at the Proceedings of WindPower 95, AWEA, Washington, D.C., 1995.
- [5] C. Kong, T. Kim, D. Han, and Y. Sugiyama, "Investigation of fatigue life for a medium scale composite wind turbine blade," *International Journal of Fatigue*, vol. 28, p. 6, 2006.
- [6] Y. J. Jang, C. W. Choi, J. H. Lee, and K. W. Kang, "Development of fatigue life prediction method and effect of 10-minute mean wind speed distribution on fatigue life of small wind turbine composite blade," *Renewable Energy*, vol. 79, p. 12, 2014.
- [7] R. P. L. Nijssen, "Fatigue Life Prediction and Strength Degradation of Wind Turbine Rotor Blade Composites," PhD, Delft University of Technology, Delft, The Netherlands, 2007.
- [8] D. A. Spera, presented at the Windpower 93, Washington DC, 1993.
- [9] D. Cárdenas, H. Elizalde, P. Marzocca, S. Gallegos, and O. Probst, "A coupled aeroelastic damage progression model for wind turbine blades," *Composite Structures*, vol. 94, p. 9, 2012.
- [10] J. Jonkman, W. Butterfield, W. Musial, and G. Scott, "Definition of a 5-MW Reference Wind Turbine for Offshore System Development," National Renewable Energy Laboratory, Colorado, USA2009.
- [11] B. R. Resor, "Definition of a 5MW/61.5m Wind Turbine Blade Reference Model," Sandia National Laboratories, Albuquerque, New Mexico2013.
- [12] O. Castro, M. Lennie, G. Pechlivanoglou, C. N. Nayeri, and C. O. Paschereit, "The use of a new fatigue tool (ALBdeS) to analyse the effects of vortex generators on wind turbines," presented at the Proceedings of ASME Turbo Expo 2015: Turbine Technical Conference and Exposition, Montreal, Canada, 2015.
- [13] V. A. Passipoularidis, T. P. Philippidis, and P. Brondsted, "Fatigue life prediction in composites using progressive damage modelling under block and spectrum loading," *International Journal of Fatigue*, vol. 33, pp. 132-144, 2// 2011.
- [14] J. Jonkman and M. Buhl, "FAST User's Guide," National Renewable Energy Laboratory2005.
- [15] T. Kim, A. M. Hansen, and K. Branner, "Development of an anisotropic beam finite element for composite wind turbine blades in multibody system," *Renewable Energy*, vol. 59, p. 11, 2013.
- [16] J. Jonkman, S. Butterfield, P. Passon, T. Larsen, T. Camp, J. Nichols, *et al.*, "Offshore Code Comparison Collaboration within IEA Wind Annex XXIII: Phase II Results Regarding Monopile Foundation Modeling," presented at the IEA European Offshore Wind Conference, Berlin, Germany, 2007.
- [17] J. P. Blasques and M. Stolpe, "Multi-material topology optimization of laminated composite beam cross sections," *Composite Structures*, vol. 94, p. 11, 2012.

- [18] R. D. Bitsche, "Airfoil2BECAS: A preprocessor for the cross-section analysis software BECAS," Technical University of Denmark, Roskilde, Denmark 2014.
- [19] M. L. Buhl, "Crunch user's guide," National Renewable Energy Laboratory, Golden, Colorado 2003.
- [20] A. Nieslony, "Determination of fragments of multiaxial service loading strongly influencing the fatigue of machine components," *Mechanical Systems and Signal Processing*, vol. 23, p. 9, 2009.
- [21] A. Palmgren, "Die Lebensdauer von Kugellagern," *Zeitschrift von Deutsche Ingenieurring*, vol. 68, p. 3, 1924.
- [22] M. Miner, "Cumulative damage in fatigue," *Journal of Applied Mechanics*, vol. 12A, p. 5, 1945.
- [23] E. Hau, *Wind Turbines: Fundamentals, Technologies, Application, Economics*, 2nd ed.: Springer, 2005.
- [24] *Wind Measurement International*. Available: <http://www.windmeasurementinternational.com/index.php>
- [25] P. Passon, M. Kühn, S. Butterfield, J. Jonkman, T. Camp, and T. J. Larsen, "OC3–Benchmark Exercise of Aero-elastic Offshore Wind Turbine Codes," *Journal of Physics*, vol. 75, 2007.